TRPM2-mediated extracellular Ca^{2+} entry promotes acinar cell necrosis in biliary acute pancreatitis

Júlia Fanczal* [1], Petra Pallagi* [1,2], Marietta Görög [1,2], Gyula Diszházi [3], János Almássy [3], Tamara Madácsy [1,2], Árpád Varga [1,2], Péter Csernay-Biró [1], Xénia Katona [1,2], Emese Tóth [1], Réka Molnár [1], Zoltán Rakonczay Jr. [4], Péter Hegyi [5,6], József Maléth [1,2,7]

[1] First Department of Medicine, University of Szeged, Szeged, Hungary

[2] HAS-USZ Momentum Epithelial Cell Signalling and Secretion Research Group, University of Szeged, Szeged, Hungary

[3] Department of Physiology, University of Debrecen, Debrecen, Hungary

[4] Department of Pathophysiology, University of Szeged, Szeged, Hungary

[5] HAS-USZ Momentum Translational Gastroenterology Research Group, University of Szeged, Szeged, Hungary

[6] Institute for Translational Medicine and First Department Medicine, Medical School, University of Pécs, Pécs, Hungary

[7] Department of Public Health, University of Szeged, Szeged, Hungary

* These authors contributed equally.

Short title: The pathogenetic role of TRPM2 in biliary pancreatitis

Correspondence to

Jozsef Maleth MD, Ph.D.

ORCID ID.: 0000-0001-5768-3090

HAS-USZ Momentum Epithelial Cell Signalling and Secretion Research Group

First Department of Medicine and Department of Public Health

University of Szeged, H6720, Szeged; Hungary

Phone: +36 (62) 342-877; +36 70 41 66500

This is an Accepted Article that has been peer-reviewed and approved for publication in the The Journal of Physiology, but has yet to undergo copy-editing and proof correction. Please cite this article as an 'Accepted Article'; doi: 10.1113/JP279047.

e-mail: jozsefmaleth1@gmail.com; maleth.jozsef@med.u-szeged-hu

Key words: TRPM2 channel, acute pancreatitis, Ca^{2+} signalling, bile acid, acinar cell necrosis, epithelial ion transport

Abbreviations: ADPR: adenosine diphosphate ribose; AP: acute pancreatitis, CDC: chenodeoxycholate, CFTR: cystic fibrosis transmembrane conductance regulator, H_2O_2: Hydrogen peroxide, NUDT9-H motif : pyrophosphatase Nudix-like domain, ROS: reactive oxygen species, TLC-S: taurolithocholic acid sulfate, TRPM2: transient receptor potential melastatin 2

KEY POINTS

- Acute biliary pancreatitis is a significant clinical challenge as currently no specific pharmaceutical treatment exists.
- Intracellular Ca^{2+} overload, increased reactive oxygen species (ROS) production, mitochondrial damage and intra-acinar digestive enzyme activation caused by bile acids are hallmarks of acute biliary pancreatitis.
- Transient Receptor Potential Melastatin 2 (TRPM2) is a non-selective cation channel that has recently emerged as an important contributor to oxidative-stress-induced cellular Ca^{2+} overload across different diseases.
- We demonstrated that TRPM2 is expressed in the plasma membrane of mouse pancreatic acinar and ductal cells, which can be activated by increased oxidative stress induced by H_2O_2 treatment and contributed to bile acid-induced extracellular Ca^{2+} influx in acinar cells, which promoted acinar cell necrosis *in vitro* and *in vivo.*
- These results suggest that the inhibition of TRPM2 may be a potential treatment option for biliary pancreatitis.

ABSTRACT

Acute biliary pancreatitis poses a significant clinical challenge as currently no specific pharmaceutical treatment exists. Disturbed intracellular Ca^{2+} signalling caused by bile acids is a hallmark of the disease, which induces increased reactive oxygen species (ROS) production, mitochondrial damage, intra-acinar digestive enzyme activation and cell death. Because of this mechanism of action, prevention of toxic cellular Ca^{2+} overload is a promising therapeutic target. Transient Receptor Potential Melastatin 2 (TRPM2) is a non-selective cation channel that has recently emerged as an important contributor to oxidative-stress-induced cellular Ca^{2+} overload across different diseases. However, the expression and possible functions of TRPM2 in the exocrine pancreas remain unknown. Here we found that TRPM2 is expressed in the plasma membrane of mouse pancreatic acinar and ductal cells, which can be activated by increased oxidative stress induced by H_2O_2 treatment. TRPM2 activity was found to contribute to bile acid-induced extracellular Ca^{2+} influx in acinar cells, but did not have the same effect in ductal cells. The generation of intracellular ROS in response to bile acids was remarkably higher in pancreatic acinar cells compared to isolated ducts, which can explain the difference between acinar and ductal cells. This activity promoted acinar cell necrosis *in vitro* independently from mitochondrial damage or mitochondrial fragmentation. In addition, bile-acid-induced experimental pancreatitis was less severe in TRPM2 knockout mice, whereas the lack of TRPM2 had no protective effect in cerulein induced acute pancreatitis. Our results suggest that the inhibition of TRPM2 may be a potential treatment option for biliary pancreatitis.

Introduction

Acute pancreatitis (AP) is one of the most common inflammatory diseases of the gastrointestinal tract (Yadav & Lowenfels, 2013), which is primarily caused by impacted gallstones or heavy alcohol consumption (Parniczky *et al.*, 2016). Despite intense efforts in both basic and clinical research, no specific pharmaceutical treatment exists, and the mortality of severe forms of AP (~10% of all cases) remains remarkably high (~28%) (Parniczky *et al.*, 2016). The 'common channel' theory of biliary pancreatitis suggests that communication between the common bile duct and the pancreatic duct may exist because of impacted gallstones. Theoretically, bile acids could reach the pancreatic ductal system and the acinar cells through this channel (Lerch & Aghdassi, 2010). Although this hypothesis

is still unproven (DiMagno *et al.*, 1982; Lerch *et al.*, 1993), several studies have shown that bile acids disturb intracellular Ca^{2+} homeostasis and trigger mitochondrial damage in the exocrine pancreas. Bile acids are known to increase the intracellular Ca^{2+} concentration ($[Ca^{2+}]_I$) in isolated pancreatic acinar (Gerasimenko *et al.*, 2006) and ductal cells (Venglovecz *et al.*, 2008) *in* vitro via Ca^{2+} release from intracellular stores, sarco-endoplasmic reticulum Ca^{2+} pump (SERCA) inhibition (Kim *et al.*, 2002) and extracellular Ca^{2+} influx (Hong *et al.*, 2011). This sustained elevation of $[Ca^{2+}]_I$ can induce intra-acinar trypsinogen activation (Halangk *et al.*, 2002; Sherwood *et al.*, 2007), mitochondrial damage (Voronina *et al.*, 2010; Maleth *et al.*, 2011) and, consequently, cell necrosis in the exocrine pancreas. In addition, Booth *et al.* demonstrated that taurolithocholic acid sulphate (TLC-S) increases intracellular and mitochondrial reactive oxygen species (ROS) production, which was dependent on increases in $[Ca^{2+}]_I$ and mitochondrial Ca^{2+} concentration (Booth *et al.*, 2011). They also showed that bile acid induced the increased generation of ROS and promoted apoptosis, whereas increased intracellular and intramitochondrial Ca^{2+} initiated necrosis.

In recent years, Transient Potential Melastatin-like 2 (TRPM2), a Ca^{2+}-permeable non-selective cation channel, has been identified to act as a cellular redox-sensor (Hara *et al.*, 2002; Di *et al.*, 2011), which plays an important role in physiological functions as well as in various diseases (Takahashi *et al.*, 2011). Activation of TRPM2 by H_2O_2 is suggested to occur indirectly through intracellular production of adenosine diphosphate ribose (ADPR), which then binds to and stimulates the C-terminal ADPR pyrophosphatase Nudix-like domain (NUDT9-H motif) of TRPM2 (Perraud *et al.*, 2005). In monocytes, Ca^{2+} influx via TRPM2 was shown to increase chemokine production, leading to enhanced neutrophil infiltration in inflammatory bowel diseases (Yamamoto *et al.*, 2008). More recently, TRPM2 has been implicated in the pathogenesis of irradiation-induced xerostomia. Liu *et al.* demonstrated that irradiation followed by increased ROS production activates TRPM2, leading to extracellular Ca^{2+} influx and a consequent loss of acinar cell function in the salivary glands (Liu *et al.*,

2013). In a downstream study, the authors also showed that irradiation activated a TRPM2-dependent mitochondrial pathway, leading to caspase-3 activation and mediated cleavage of stromal interaction molecule 1, which then attenuated store-operated Ca^{2+} entry (Liu *et al.*, 2017). In the endocrine pancreas, TRPM2 has been suggested to play a role in diabetic stress-induced mitochondrial fragmentation. Abuarab *et al.* demonstrated that ROS production induced by high glucose concentrations activates TRPM2 and triggers lysosomal membrane permeabilization, leading to Zn^{2+}-mediated mitochondrial fission (Abuarab *et al.*, 2017). These studies demonstrate the expression of TRPM2 in various epithelial cells, and this protein plays a central role in the pathogenesis of oxidative-stress-related diseases. Despite this knowledge, the expression or function of TRPM2 in exocrine pancreatic cells has never been investigated.

In this study, TRPM2 was shown to be expressed in the acinar and ductal cells of the exocrine pancreas. In both cell types, TRPM2 was also found to mediate extracellular Ca^{2+} influx during oxidative stress conditions. The non-conjugated bile acid chenodeoxycholate (CDC) was found to activate TRPM2-mediated Ca^{2+} influx in acinar cells, but did not do the same in ductal cells, contributing to acinar cell damage and increased acinar cell necrosis that was independent from mitochondrial damage. Importantly, a knockout of the gene encoding TRPM2 was found to significantly decrease tissue necrosis in an experimental model of acute biliary pancreatitis. Taken together, these results are the first description of the expression and functional activity of TRPM2 in the exocrine pancreas. Moreover, evidence was demonstrated for the important role that the activation of this channel plays in biliary pancreatitis.

Materials and Methods

Animals

TRPM2 knockout mice were generously provided by Yasuo Mori (Kyoto University; Kyoto, Japan). The knockout mice were generated from a C57BL/6 background as described previously (Yamamoto *et al.*, 2008). TRPM2 +/+ and TRPM2 −/− mice were bred from TRPM2+/− animals and were used for experiments between the age of 8–12 weeks. Mice were kept in standard 12 hour light-dark cycle and on standard rodent food ad libitum. Mice genotyped using a standard polymerase chain reaction (PCR) assay as described in (Liu *et al.*, 2013). Experiments on live animals were carried out with adherence to the NIH guidelines and the EU directive 2010/63/EU for the protection of animals used for scientific purposes. The study was authorized by the National Scientific Ethical Committee on Animal Experimentation under licence number XXI./2523/2018. Terminal anaesthesia was induced in mice with 250 mg/bwkg sodium pentobarbital. Before surgery, mice were anaesthetised with 125 mg/kg ketamine and 12.5 mg/kg xylazine. After operation the animals were placed on a heating pad until they regained consciousness, following which they were given buprenorphine (0.075 mg/kg) i.p. to reduce pain.

Isolation of pancreatic acinar cells

Pancreatic acinar cells from wild-type and TRPM2 knockout mice were isolated as described previously (Gout *et al.*, 2013). Briefly, mice were sacrificed, and the pancreas was removed and was placed into ice-cold Hank's Balanced Salt Solution (HBSS; Sigma-Aldrich; Cat. No.: 8264). The tissue was then cut into small pieces in a 1.5 mL centrifuge tube which were placed into a sterile flask with 10 mL of isolation solution [10 mL HBSS (Cat. No.: Sigma; H9269), 200 U/mL of collagenase (Worthington; Cat. No.: 5273), 10 mM HEPES (Sigma-Aldrich; Cat. No.: 3375)]. The tissue was incubated for 25–30 min at 37°C and was vigorously shaken every 5 min. After digestion, the pancreas was placed into a 50 mL tube (Sarstedt; 62.559.205) with 10 mL of ice-cold washing solution (containing 10 mL HBSS, 10 mM HEPES, 5 % Foetal Bovine Serum Cat. No.: Gibco;

10500-064) and centrifuged at 90 RCF at 4°C for 2 min. This step was repeated two times. The supernatant was removed, and the pellet was resuspended in 1 mL HBSS solution. Until experimental use, the acinar cells were kept in an incubator at 37°C with 5% CO_2.

Isolation of pancreatic ductal fragments

Isolation of inter-, and intralobular pancreatic ductal fragments was performed as described previously (Maleth *et al.*, 2015). Terminal anaesthesia was induced in mice with 250 mg/bwkg sodium pentobarbital and the removed pancreas was digested for 15 min with 100 U/mL purified collagenase (Worthington, Cat. No.: LS005273) containing solution at 37°C applying gentle shaking. The isolation solution also contained 0.1 mg/mL trypsin inhibitor (ThermoFisher Scientific, Cat. No.: 17075029) and 1 mg/mL bovine serum albumin (VWR, Cat. No.: 9048-46-8) in DMEM Nutrient Mixture F-12 Ham (Sigma, Cat. No.: D6421).. Pancreatic ducts were separated from the acinar lobules under a stereomicroscope and used for downstream analysis.

Gene expression analysis

Gene expression was investigated by the combination of reverse-transcription (RT-PCR) and conventional PCR. Total mRNA was isolated from three independent biological replicates of mouse brain, isolated pancreatic acini or isolated pancreatic ducts with the NucleoSpin RNA XS kit (Macherey-Nagel, Ref.: 740902.50) according to the manufacturer's instructions. The mRNA concentrations were measured with NanoDrop™ 2000 (ThermoFisher Scientific). 1 µg purified mRNA was used to synthetize cDNA. using an iScript™ cDNA Synthesis kit (Bio-Rad; Cat. No.: 1708890). Conventional PCR amplification was performed by DreamTaq Hot Start DNA Polymerase (ThermoFisher Scientific, Cat. No.: EP1702) with cDNA specific primers (forward: ACGGGCAATATGGTGTGGAG; reverse: CACCTCCCCTTTCCTTCGTT) for 35 cycles. Mouse brain lysate was used to validate the primers.

Immunofluorescent labelling

For immunostaining pancreatic acinar cells were isolated and attached to poly-l-lysine-coated cover glasses, whereas pancreatic ducts were frozen in Shandon Cryomatrix (ThermoFisher Scientific, Cat. No.: 6769006) and 7 µm thick sections were cut with a cryostat (Leica CM 1860 UV). Antibody labelling was performed as previously described (Molnar *et al.*, 2019). Briefly, sections were fixed in 4% PFA-PBS and after antigen retrieval with sodium citrate–Tween 20 buffer sections were blocked for 1 h. Sections were incubated with Anti-TRPM2-ATTO-594 (Alomone Labs Cat. No.: ACC-043-AR) conjugated primary rabbit polyclonal antibody overnight at 4°C (1:100 dilution). Nuclei were labelled with Hoechst 33342 and sections were kept in a Fluoromount mounting medium (Sigma-Aldrich; Cat. No.: F4680) until imaging. Sections were imaged with a Zeiss LSM880 laser scanning confocal microscope using a 40× oil immersion objective (Zeiss, NA: 1.4).

Electrophysiology

For electrophysiology recordings, pancreatic acinar cells were isolated from mouse pancreas as described previously (Geyer *et al.*, 2015), with slight modifications. The pancreas was removed and injected with a F12/DMEM (ThermoFisher Scientific Cat. No.: 11320033) medium containing 100 U/mL collagenase P (Roche), 0.1 mg/mL trypsin inhibitor and 2.5 mg/mL BSA. These were then incubated in 5 mL volume of the same solution in a 37°C shaking water bath for 30 min, which was continuously gassed with carbogen. The tissue was dissociated by pipetting with a serological pipette 4–6 times before filtering through a 150 µm mesh. Cells were layered on top of 400 mg/mL BSA and washed through the medium by gentle centrifugation. The pellet was resuspended in Ca^{2+}-free, collagenase-containing Tyrode's solution before being further digested for 10 min. Following this, cell clumps were gently agitated with a 1 mL pipette tip attached to a serological pipette. The

resulting cells were collected by centrifugation, resuspended in DMEM medium and kept gassed at room temperature until use in patch clamp experiments. Whole cell currents were acquired at room temperature using an Axopatch 200B amplifier and a Digidata 1322A digitiser (Axon Instruments) at a 50 kHz sampling rate and filtered online at 5 kHz using a low-pass Bessel filter. Data acquisition was performed using pClamp 9 software package (Axon Instruments). Pipettes of ~6 MΩ resistance were used with the intracellular solution containing 130 mM Cs-glutamate, 5 mM $CaCl_2$, 10 mM EGTA (resulting in 135 nM ionised Ca^{2+}), 5 mM $MgCl_2$ and 10 mM HEPES, pH: 7.3. Pancreatic acinar cells were continuously perfused with extracellular saline solution (140 mM Na-glutamate, 4 mM CsCl, 2 mM $CaCl_2$, 2 mM $MgCl_2$, 10 mM HEPES, pH: 7.4) with or without 100 µM H_2O_2. Cation currents were recorded during 100 ms long test pulses at step potentials between −60 and +120 mV both under control conditions and during treatment.

Fluorescent microscopy

Isolated pancreatic acinar clusters or ductal fragments were placed on poly-l-lysine-coated cover glasses and incubated with BCECF-AM (1.5 µmol/L) or Fura2-AM (5 µmol/L) for 30 min at 37°C (Hegyi *et al.*, 2004). The loaded cells were imaged with an Olympus IX71 inverted microscope equipped with a Hamamatsu ORCA-ER CCD camera through a 20× oil immersion objective (Olympus; NA: 0.8). Samples were excited with an Olympus MT-20 illumination system equipped with a 150 W xenon arc light source. Filter combinations for BCECF and Fura2 was described previously (Molnar *et al.*, 2019). . Ratiometric image analysis was performed using Olympus excellence software with a temporal resolution of 1 s.

Investigation of acinar cell fate

To investigate acinar cell fate, an apoptosis/necrosis detection kit was used according to the manufacturer's instruction (Abcam Cat. No.: ab176750). CytoCalcein Violet 450 is sequestered in the

cytoplasm of live cells. In apoptosis, phosphatidylserine (PS) is transferred to the outer leaflet of the plasma membrane, which can be detected by the PS sensor Apopxin Deep Red. During necrosis the cell membrane integrity is lost and thus the DNA Nuclear Green DCS1, a membrane-impermeable dye can label the nucleus of damaged cells. Briefly, pancreatic acinar cells from wild-type (WT) and TRPM2 KO mice were isolated as described above with modifications to improve overall cell survival (shorter tissue digestion and gentle centrifugation was applied) and incubated with 1 mM H_2O_2 or 250 µM CDC for 30 min. Cells were then centrifuged at 500 RCF for 5 min at 4°C and washed twice with PBS. Cells were then resuspended in 200 µL of Assay Buffer and loaded with CytoCalcein 450, Nuclear Green and Apopxin Deep Red at room temperature for 30–60 min. Following this, cells were collected and centrifuged at 500 RCF for 5 min at 4°C before being placed on a Cellview cell culture slide (Greiner Bio-One cat. no.: 543979) for imaging. Images were captured using a Zeiss LSM880 confocal microscope with different channels and wavelengths according to each dye: CytoCalcein 450 (Ex/Em = 405/450 nm), Nuclear Green (Ex/Em = 490/520 nm) and Apopxin Deep Red (Ex/Em = 630/660 nm). For each condition, five images were captured, and the total number of cells was counted by two independent investigators. Cells with Nuclear Green staining were considered necrotic, with Apopxin Deep Red staining apoptotic, whereas double stained cells were considered necrotic.

Confocal imaging of live acinar cells

Changes of the mitochondrial membrane potential ($\Delta\Psi_m$) were followed by using tertamethylrhodamine-methyl ester (TMRM), which accumulates in the mitochondria depending on $\Delta\Psi_m$. Generation of intracellular ROS was measured by H2DCFDA ROS indicator. Isolated pancreatic acinar cells were incubated with 100 nM TMRM (ThermoFisher Scientific Cat. No.: T668), or 4 µM H2DCFDA (ThermoFisher Scientific Cat. No.: D399) in standard HEPES solution for 20 min at 37°C on a poly-l-lysine-coated cover glass. The solutions were complemented with 100 nM

TMRM to avoid dye leakage. Changes in $\Delta\Psi_m$ or intracellular ROS were monitored using a ZEISS LSM880 confocal microscope. The cells loaded with TMRM were excited with 543 nm, and the emitted light was captured between 560 and 650 nm. Five to 10 ROIs were placed on the mitochondria of pancreatic acinar cells. H2DCFDA was excited with 490 nm and the emitted fluorescence was captured between 500 and 550 nm. Fluorescence signals were normalised to initial fluorescence intensity (F/F_0) and expressed as relative fluorescence.

***In vivo* acute pancreatitis models**

Cerulein-induced acute pancreatitis (AP) was induced by 10, hourly intraperitoneal injections of 50 µg/bwkg cerulein (Bachem Cat. No.: H-3220) (control groups received physiological saline) (Pallagi *et al.*, 2014). Two hours after the last cerulein injection, mice were euthanised with 85 mg/kg pentobarbital. Biliary AP was triggered by the administration of 4% Na-taurocholate (Sigma-Aldrich Cat. No.: 86339) into the common bile duct as described previously by Perides et al. (Perides *et al.*, 2010b). Briefly, mice were anaesthetised with 125 mg/kg ketamine and 12.5 mg/kg xylazine, and median laparotomy was performed, where the papilla of Vater was cannulated by a 0.4 mm diameter needle connected to an infusion pump. Mice were administered 4% Na-taurocholate or physiological saline at a perfusion rate of 10 µL/min [TSE System GmbH-cat. no.: 540060-HP] for 5 min. After the abdominal wall and the skin were closed separately, the animals were placed on a heating pad until they regained consciousness, following which they were given buprenorphine (0.075 mg/kg) i.p. to reduce pain. Mice were sacrificed 24 h later using pentobarbital (85 mg/kg i.p.). In both cases, blood samples were collected after terminal anaesthesia through the inferior vena cava, and the pancreata were removed immediately. Blood samples were placed on ice and then centrifuged at 2500 RCF for 15 min at 4°C. Serum samples were collected and stored at −20°C. Pancreas samples were placed into a 4% formaldehyde solution and stored at 4°C until histology. A colorimetric kit (A Amylase Assay) was used to measure serum amylase activity (Diagnosticum, Cat. No.: 47462). Absorbance of the

samples was detected at 405 nm using a FLUOstar OPTIMA (BMG Labtech) microplate reader. Formaldehyde-fixed pancreas samples were embedded in paraffin, and 4 μm thick sections were cut and stained with haematoxylin–eosin. Histologic parameters such as oedema, inflammatory cell infiltration and necrosis were scored (0–5 points for oedema, leukocyte infiltration and necrosis for the total histological score, or % of total area for necrosis) by three independent investigators blinded to the protocol (Pallagi *et al.*, 2014). Averages of the scores were calculated and included to the manuscript. Total histological score was calculated by adding the individual scores together.

Statistics

Statistical analysis was performed by Graphpad Prism software. All data are expressed as means ± SD. Both parametric (one-way analysis of variance) and nonparametric (Mann Whitney test, Kruskal-Wallis test - for analysis of the acinar cell survival assay) tests were used based on the normality of data distribution. A p value of less than 0.05 was accepted as statistically significant.

Results

TRPM2 channel is expressed in the exocrine pancreas

End-point PCR analysis of isolated acini and ductal fragments confirmed that the TRPM2 gene was expressed in the exocrine pancreatic cells (Figure 1.A.). When immunofluorescent labelling of TRPM2 was performed on isolated acinar clusters and cross sections of isolated ducts, the confocal images showed that TRPM2 channels were expressed on the basolateral membrane of the pancreatic acinar cells, whereas an apical expression pattern was seen in ductal cells (Figures 1.B–C).

Functional TRPM2 channels are present in pancreatic acinar and ductal cells

When isolated WT pancreatic acini were challenged with 1 mM H_2O_2 to increase ROS, a rapid and sustained increase of $[Ca^{2+}]_I$ was observed (Figure 2.A), which was significantly reduced in the

TRPM2 knockout (KO) acini (0.41 ± 0.09 vs 0.17 ± 0.029, respectively). In cells treated in an extracellular Ca^{2+}-free medium, Ca^{2+} elevation was found to be significantly impaired, and no difference was detected between WT and TRPM2 KO cells. This suggests that the sustained elevation of $[Ca^{2+}]_I$ in response to H_2O_2 was largely due to TRPM2-channel-mediated influx of extracellular Ca^{2+}. In addition, H_2O_2 activated a reversible cationic membrane current, with a relative linear I–V relationship as was reported previously for TRPM2 (Liu *et al.*, 2013) (Figure 2.B). Similarly to acinar cells, treatment of isolated WT pancreatic ductal fragments with 1 mM H_2O_2 induced a sustained elevation of $[Ca^{2+}]_I$ (Figure 2.C), which was significantly lower in TRPM2 KO ductal cells (0.30 ± 0.06 vs 0.10 ± 0.013, respectively). In these cells as well, Ca^{2+} elevation was significantly lower in Ca^{2+}-free conditions (Figure 2.C.). As the intracellular Ca^{2+} level of pancreatic ductal cells decrease in response to extracellular Ca^{2+} removal, we normalised the maximal Ca^{2+} responses to the same initial value. Genetic inhibition of TRPM2 channels had no effect on amylase release from pancreatic acinar cells (data not shown) or on the HCO_3^- secretion by pancreatic ductal cells (described below, Figures 3.C–D). Therefore, the physiological relevance and function of TRPM2 in the exocrine pancreas still require further characterisation and study.

TRPM2 contributes to bile-acid-induced extracellular Ca^{2+} influx in pancreatic acinar cells

Bile acids can cause the release of Ca^{2+} from intracellular stores and can trigger extracellular Ca^{2+} influx. To study this, the intracellular Ca^{2+} elevation in response to bile acid treatment was compared in pancreatic acini and ducts. Administration of 250 μM CDC was found to trigger a rapid, sustained increase in $[Ca^{2+}]_I$, which was markedly impaired in the TRPM2 KO acinar cells (0.834 ± 0.02 vs 0.655 ± 0.04) (Figure 3.A). These results highlight that TRPM2 plays an important role in bile-acid-induced extracellular Ca^{2+} influx in pancreatic acinar cells. By contrast, no significant difference was detected in isolated ductal fragments between the Ca^{2+} response of WT and TRPM2 KO ducts to 250

μM CDC, suggesting that, in ductal cells, TRPM2 plays no role in bile-acid-induced cell injury (Figure 3.B).

Since HCO_3^- secretion is the primary function of the ductal epithelia, the HCO_3^- efflux across the apical membrane was compared between WT and TRPM2 KO ducts using fluorescent intracellular pH (pH_i) measurements (Maleth *et al.*, 2015). Ductal cells were exposed to 20 mM NH_4Cl in HCO_3^-/CO_2-buffered solution from the basolateral membrane, triggering a rapid alkalisation because of the influx of NH_3 (Figure 3.D), followed by a slower recovery of the alkaline pH to the resting pH_i. This recovery phase depends on the HCO_3^- efflux (i.e. secretion) from the ductal epithelia via the SLC26 Cl^-/HCO_3^- exchangers and CFTR (Maleth *et al.*, 2015). Removal of NH_4Cl rapidly decreased pH_i below the resting value, which is restored by the activities of the basolateral NHE1 and NBCe1 (Maleth *et al.*, 2015). The initial recovery rates were measured (calculated as $\Delta pH/\Delta t$) over the first 30 s to calculate the base flux [$J(B^-)$] values as described (Maleth *et al.*, 2015). With this assay, no difference in the activities of the apical and basolateral proteins was found between WT and TRPM2 KO ducts (Figures 3.D-E). Although the administration of CDC markedly inhibited ion secretion as has been previously described (Maleth *et al.*, 2011), the genetic knockout of TRPM2 demonstrated no protective effect, suggesting that bile acids affect ductal cells via a TRPM2-independent mechanism (Figures 3.D-E).

To provide mechanistic explanation for the different contribution of TRPM2 in bile acid generated Ca^{2+} response in acinar and ductal cells, we measured the intracellular ROS using H2DCFDA. In accord with the previous findings of Booth et al. (Booth *et al.*, 2011), we showed that 250 μM CDC increased the intracellular ROS level in pancreatic acini. Interestingly, the ROS production during bile acid treatment in ductal epithelial cells was significantly lower compared to acinar cells (13.6±2 vs 33.4±4 arbitrary unit).

Lack of TRPM2 decreases acinar cell necrosis during bile acid exposure

Pancreatic acinar cell fate determines the severity of AP. Because of this, it was also important to characterise the role of TRPM2 in acinar cell death. In the untreated control samples, ~85% of the acinar cells were viable in both the WT and TRPM2 KO samples, which is comparable to previously published results (Booth *et al.*, 2011). Incubation of WT and TRPM2 KO acini with 1 mM H_2O_2 for 30 min remarkably decreased the number of viable cells, and necrotic cell death was significantly increased (Figure 4.A-B). A lack of TRPM2 was observed to protect acinar cells from oxidative-stress-induced cell necrosis during H_2O_2 treatment (% of viable cells: 19.4 ± 0.4 in WT vs 49.1 ± 1.2 in TRPM2 KO). The rate of apoptosis was similar in TRPM2 KO and WT acini (% of apoptotic cells: 9.1 ± 4.3 in WT vs 10.8 ± 2.5 in TRPM2 KO), whereas necrosis was significantly impaired in TRPM2 KO acini (% of necrotic cells: 71.5 ± 4.2 in WT vs 40.1 ± 3.2 in TRPM2 KO). Similarly, incubation of acinar cells with 250 μM CDC for 30 min decreased the number of live cells in WT sample, however overall cell survival was remarkably improved by TRPM2 deletion (% of viable cells: 48.3 ± 0.9 in WT vs 74.1 ± 1.3 in TRPM2 KO) (Figure 4.A-B). TRPM2 deletion significantly decreased booth apoptotic and necrotic cell death in the CDC treated group (WT: 15.4 ± 2.5% vs KO: 8.5 ± 1.3% and WT: 36.3 ± 2.2% vs KO:17.4 ± 1.3%, respectively). Importantly, the lack of TRPM2 channels resulted in a ~30% decrease in acinar cell death, suggesting that TRPM2 has an important contribution to acinar cell death during biliary AP.

Lack of TRPM2 does not prevent mitochondrial damage during bile acid exposure

We wanted to further characterise the intracellular mechanisms that play a role in TRPM2-channel-mediated cell necrosis. As TRPM2 has been reported to induce mitochondrial damage (Liu *et al.*, 2017), the mitochondrial membrane potential was measured ($\Delta\psi_m$) in WT and TRPM2 pancreatic acinar cells. Administration of 1 mM H_2O_2 resulted in a marked drop of $\Delta\psi_m$ in WT cells (Figure 5.A). The decrease of $\Delta\psi_m$ was significantly lower in TRPM2 KO cells, whereas removal of the

extracellular Ca^{2+} impaired the loss of $\Delta\psi_m$ in WT cells to the level of TRPM2 KO acini. This suggests that extracellular Ca^{2+} influx through TRPM2 plays a crucial role in the oxidative-stress-induced mitochondrial damage seen in pancreatic acinar cells. The decrease of $\Delta\psi_m$ in response to 250 µM CDC was also compared. However, no difference was seen between WT and TRPM2 KO cells (Figure 5.B). This may be due to the Ca^{2+}-independent direct mitochondrial toxicity of bile acids (Schulz *et al.*, 2013). Previously, TRPM2 channels have been suggested to be key mediators of diabetic stress-induced mitochondrial fragmentation in endothelial cells (Abuarab *et al.*, 2017). Notably, in pancreatic acinar cells, fragmentation of mitochondria was not observed in response to either H_2O_2 or bile acid treatment (Figure 5.C).

Lack of TRPM2 decreases the severity of experimental biliary pancreatitis

To determine the role of TRPM2 in the pathogenesis of AP, the disease severity of WT and TRPM2 KO animals was compared in two standard experimental AP models. In the first series of experiments, mice were given 10 hourly i.p. injections of either physiological saline (control group) or 50 µg/bwkg cerulein to induce AP (Figure 6.A). Overall, in this experimental model, no significant differences were detected between WT and TRPM2 KO mice. The control animals had normal pancreatic histology in both groups (Figure 6.A), whereas cerulein hyperstimulation caused extensive pancreatic damage. Despite this, no significant differences were observed in the histological parameters between the WT and TRPM2 KO animals. The extent of interstitial oedema (3.14 ± 0.25 for WT vs 3.03 ± 0.34 for KO), leukocyte infiltration (2.74 ± 0.53 for WT vs 3.04 ± 0.23 for KO, $p = 0.08$) or necrosis (18.64 ± 3.16 for WT vs 21.32 ± 3.58 for KO) was not found to be significantly different in the cerulein-treated groups (Figure 6.B).

More importantly, the role of the TRPM2 channel in the pathogenesis of biliary AP was also examined. In this model, pancreatitis was induced by intraductal infusion of 4% Na-taurocholate (TC) (control animals received physiological saline) as described previously (Pallagi *et al.*, 2014). The

infusion of 4% Na-taurocholate induced necrotising pancreatitis in both WT and TRPM2 KO mice, accompanied by elevated histological and laboratory parameters (Figures 6.C–D). The extent of interstitial oedema (2.8 ± 0.16 for WT vs 2.7 ± 0.2 for KO) or leukocyte infiltration (3.3 ± 0.38 for WT vs 2.7 ± 0.29 for KO, p = 0.08) was not significantly different in the Na-taurocholate-treated groups. Notably, the extent of necrosis was significantly higher in the WT group in comparison to the TRPM2 KO animals (41.3% ± 7.13% for WT vs 26.4% ± 5.5% for KO). In accordance with these findings, serum amylase activities were also significantly higher in the Na-taurocholate-treated WT animals versus the TRPM2 KO group. This perfectly mimicked the *in vitro* results obtained in this study, further confirming the crucial role of the TRPM2 channel in the pathogenesis of biliary AP.

Discussion

Previous reports suggest that bile acids can trigger sustained intracellular Ca^{2+} elevation, increase intracellular and intramitochondrial ROS production and damage the mitochondrial network in both pancreatic acinar and ductal cells. These subcellular changes can eventually lead to AP, which is a severe inflammatory disease of the gastrointestinal tract that has no specific treatment. Although the TRPM2 channel has recently emerged as a ROS-sensitive non-specific cation channel which mediated Ca^{2+}-dependent injury, the possible role that this channel plays in the pathogenesis of AP has yet to be investigated.

Though the expression of TRPM2 has been demonstrated previously in different cell types, including inflammatory cells (Yamamoto *et al.*, 2008), myocytes (Miller *et al.*, 2019) and epithelial cells (Liu *et al.*, 2013), to our knowledge, this is the first report demonstrating the expression of TRPM2 in the exocrine pancreas. Using conventional PCR and immunolabelling techniques, the expression of TRPM2 in the basolateral membrane of acinar cells and on the luminal membrane of ductal cells was confirmed. In addition, increased intracellular ROS was found to trigger TRPM2-mediated extracellular Ca^{2+} influx in both cell types. This study did not show any alterations in acinar and

ductal cell function between WT and TRPM2 KO mice. However, intracellular Ca^{2+} signalling is one of the major signalling pathways in the exocrine pancreas (Ahuja *et al.*, 2014; Maleth & Hegyi, 2014) which regulates the secretion of digestive enzymes in acinar cells as well as ion and fluid secretion in ductal cells. Therefore, it might be possible that TRPM2-mediated Ca^{2+} entry could contribute to physiological signalling, though further studies are required in order to confirm this. In other cell types, redox signals have been demonstrated to sensitise TRPM2 and increase the intracellular Ca^{2+} concentration at physiological body temperature, which plays an important role in the regulation of macrophage functions (Kashio *et al.*, 2012). In TRPM2 KO mice, blood glucose levels were significantly higher, whereas insulin secretion was significantly impaired, suggesting a potential role of TRPM2-mediated Ca^{2+} increase in insulin secretion (Uchida *et al.*, 2011). On the other hand, activation of TRPM2 channels in pancreatic β-cells increased intracellular Ca^{2+} concentration and release of sequestered intracellular Zn^{2+} from lysosomes (Manna *et al.*, 2015). In these experiments, gene knockout of TRPM2 protected mice from β-cell death. Previously, TRPM2 facilitated extracellular Ca^{2+} influx in monocytes in response to H_2O_2 and thus regulated the production of the macrophage inflammatory protein-2 (CXCL2), which, in turn, regulated the inflammatory response in a dextran sulphate sodium-induced colitis inflammation model in mice (Yamamoto *et al.*, 2008). In another experimental model, the lack of TRPM2-regulated CXCL2 production in TRPM2 KO mice suppressed neutrophil infiltration into the central nervous system and slowed the progression of experimental autoimmune encephalomyelitis (Tsutsui *et al.*, 2018). The role of TRPM2 has also been indicated in irradiation-induced side effects in cancer patients. In salivary gland epithelial cells, irradiation increased ROS production during radiotherapy of head and neck cancers, which activated TRPM2-mediated extracellular Ca^{2+} influx in acinar cells (Liu *et al.*, 2013). The sustained intracellular Ca^{2+} entry leads to impaired secretory function of acinar cells and to the development of xerostomia–a frequent side effect of radiotherapy in these patients. In a downstream study, the same group demonstrated that irradiation increased the mitochondrial Ca^{2+} concentration and the production

of ROS, impaired the $\Delta\psi_m$ and activated caspase-3. These changes lead to a sustained decrease in STIM1 expression and consequently decreased the store-operated Ca^{2+} entry (Liu *et al.*, 2017).

Disturbed intracellular Ca^{2+} homeostasis has been suggested by several studies to play a pivotal role in bile-acid-induced exocrine pancreatic cell damage. In pancreatic acini, bile acids trigger dose-dependent intracellular Ca^{2+} elevation via the activation of IP_3 and ryanodine receptors (Gerasimenko *et al.*, 2006). In addition, Perides et al. showed that activation of the G-protein-coupled cell surface bile acid receptor (Gpbar1 or TGR5) at the apical membrane of pancreatic acinar cells leads to sustained Ca^{2+} elevation, intracellular activation of digestive enzymes and cell injury (Perides *et al.*, 2010a). Moreover, the genetic deletion of Gpbar1 specifically reduced the severity of TLCS-induced AP. On the other hand, however, in pancreatic ductal cells, CDC dose-dependently elevated the intracellular Ca^{2+} level and inhibited HCO_3^- secretion (Venglovecz *et al.*, 2008). In our experiments, CDC increased the $[Ca^{2+}]_I$ both in acinar and ductal cells, but genetic deletion of TRPM2 decreased Ca^{2+} elevation only in acinar cells. The results of this study show that the TRPM2 channel has a ~22% contribution to the bile-acid-generated Ca^{2+} signal in acinar cells. Interestingly, our results highlighted that the generation of intracellular ROS in response to bile acids is remarkably different in pancreatic acinar and ductal cells, which can provide mechanistic explanation for the different involvement of TRPM2 in bile acid generated Ca^{2+} response in these cell types. This different response might be caused by the difference in the mitochondrial mass in acinar versus ductal cells (Park *et al.*, 2001; Maleth *et al.*, 2011). As expected from this, the genetic deletion of TRPM2 had no protective effect against bile-acid-induced inhibition of ductal secretion. Whereas in acini, other plasma membrane Ca^{2+} channels were also demonstrated to contribute to cell damage during AP. Gerasimenko et al. showed that the inhibition of extracellular Ca^{2+} entry via Orai1 decreases acinar cell necrosis *in vitro* (Gerasimenko *et al.*, 2013). Moreover, inhibition of Orai1 by selective inhibitors markedly impaired the extracellular Ca^{2+} influx and sustained Ca^{2+} overload in pancreatic acinar cells upon bile acid

stimulation, which significantly impaired pancreatic oedema, inflammation and necrosis in experimental models of AP (Wen *et al.*, 2015). Others found that deletion of TRPC3 markedly reduced the bile-acid-evoked Ca^{2+} signals and decreased the intracellular trypsin activation *in vitro* and the severity of cerulein-induced AP *in vivo* (Kim *et al.*, 2009). In addition, Kim et al. described that transporter-mediated bile acid uptake results in a specific and significant of the sarco/endoplasmic reticulum Ca^{2+} ATPase pump function and thus deplete the endoplasmic reticulum Ca^{2+} stores leading cell damage and necrosis (Kim *et al.*, 2002).

Intracellular Ca^{2+} overload can lead to premature activation of trypsinogen (Kruger *et al.*, 2000), mitochondrial damage and cell necrosis in acinar cells (Criddle *et al.*, 2006). In this study, a knockout of TRPM2 resulted in a significant protection of pancreatic acinar cells from H_2O_2 and bile-acid-induced necrosis. Importantly, this protection was also observed in TC-induced AP as the extent of necrosis was significantly lower in TRPM2 knockout mice compared to the WT littermates. In line with our results, in a previous study, Booth et al. reported that incubation of pancreatic acinar cells with TLC-S *in vitro* induced Ca^{2+}-dependent necrosis, which was abolished by BAPTA-AM pre-treatment (Booth *et al.*, 2011). Using different inhibitors to prevent apoptosis and necrosis, the authors suggested that elevated intracellular and intramitochondrial ROS are the major triggers of apoptosis, whereas increases in intracellular and intramitochondrial Ca^{2+} induce necrosis. As bile acids inhibited cellular ATP production (Voronina *et al.*, 2010) and decreased $\Delta\Psi_m$ (Voronina *et al.*, 2004), we also compared the changes of $\Delta\Psi_m$ in response to bile acid treatment in TRPM2 KO and WT acinar cells. The genetic knockout of TRPM2 and removal of the extracellular Ca^{2+} markedly reduced the drop of $\Delta\psi_m$, suggesting that extracellular Ca^{2+} influx through TRPM2 plays a crucial role in oxidative-stress-induced mitochondrial damage. Despite this, we did not detect this protective effect in bile-acid-treated cells a result which might be explained by the Ca^{2+}-independent direct mitochondrial toxicity of bile acids. Direct mitochondrial toxicity of bile acids was described in an experimental model of

cholestasis. In these series of experiments Schultz et al. found that bile acids impaired the mitochondrial membrane potential and induced mitochondrial permeability transition pore opening (Schulz *et al.*, 2013). Another group showed that physiologically relevant concentrations of bile acids can induce alterations in the mitochondria outer membrane (MOM) order, which again can lead to the opening of the mitochondrial membrane permeability transition pore in isolated mitochondria (Sousa *et al.*, 2015). Previously, we (Venglovecz *et al.*, 2008) and others also reported (Voronina *et al.*, 2004) that the toxic effects of bile acids cannot be completely abolished by the removal of intracellular Ca^{2+} elevation. Mitochondrial fragmentation, which has been previously linked to the activation of TRPM2 (Abuarab *et al.*, 2017), was not observed in our experiments. These results suggest that bile acids can induce mitochondrial damage in several different ways independently form intracellular Ca^{2+} overload. On the other hand, independently from mitochondrial damage, other Ca^{2+}-dependent toxic effects of bile acids have been described, which could also contribute to acinar cell necrosis. Bile acids were shown to activate calcineurin via the elevation of intracellular Ca^{2+} in pancreatic acinar cells, leading to intra-acinar activation of chymotrypsinogen and NF-κB activation, and acinar cell death (Muili *et al.*, 2013b). In addition, genetic or pharmacological inhibition of calcineurin reduced the severity of TLC-S-induced AP, and pharmacologic and genetic inhibition of calcineurin abolished the translocation of protein kinase C, which is a critical upstream regulator of NF-κB activation (Muili *et al.*, 2013a).

In our study general TRPM2 knockout mice were used, therefore other factors might contribute to the observed protective effect of TRPM2 deletion in acute biliary pancreatitis. It is well described that inflammatory cells contribute to the severity of acute pancreatitis (Sendler *et al.*, 2018; Sendler *et al.*, 2019). Previously, TRPM2 was identified as a crucial contributor of monocyte response to oxidative stress, which in turn regulated the production of the macrophage inflammatory protein-2 (CXCL2) and inflammatory response in experimental colitis in mice (Yamamoto *et al.*, 2008). Although

inflammatory cell infiltration of the damaged area peaks several days (on day 3-4) after the initial injury, therefore these cell types do not contribute to the early events in acute pancreatitis pathogenesis. In our series of experiments, the animals were sacrificed 24 hours after the bile acid infusion, therefore we concluded that the observed difference is primarily due to the lack of TRPM2 expression in the acinar cells.

Taken together, to the best of our knowledge, this is the first report of the expression and pathological function of the TRPM2 channel in the exocrine pancreas. We demonstrated that both pancreatic acinar and ductal cells express functionally active TRPM2, which can be activated by increased oxidative stress. Importantly, we also provided evidence that TRPM2 activity contributes to bile-acid-induced extracellular Ca^{2+} influx in acinar but not ductal cells, which promotes acinar cell necrosis independently from mitochondrial damage and increases the severity of bile-acid-induced experimental pancreatitis. These results suggest that inhibition of TRPM2 might be a potential option for use in treating biliary pancreatitis.

Competing interests: The authors have no conflict of interest to declare.

Author contributions

PP and JM designed the research project; JF, MG, GyD, JA, TM, ÁV, PCSB, ET, RM, XK HP and RZ contributed to acquisition, analysis and interpretation of data for the work; PP and JM drafted the work, HP and RZ revised the manuscript critically for important intellectual content. All of the authors revised the final version of the manuscript. All authors approved the final version of the manuscript, agree to be accountable for all aspects of the work in ensuring that questions related to the accuracy or integrity of any part of the work are appropriately investigated and resolved. All persons designated as authors qualify for authorship, and all those who qualify for authorship are listed.

Funding

The research was supported by funding from the Hungarian National Research, Development and Innovation Office (PD115974 and GINOP-2.3.2–15–2016–00048 to JM, PD116553 to PP, K119938 to RZ), the Ministry of Human Capacities (EFOP 3.6.2-16-2017-00006 to JM), Bolyai Research Fellowship (BO/00440/16/5 to JM, BO/00569/17 to PP), the Hungarian Academy of Sciences (LP2017–18/2017 to JM), by the National Excellence Programme (20391-3/2018/FEKUSTRAT to JM), by the New National Excellence Program of the Ministry of Human Capacities (UNKP-18-4-SZTE-85 to PP, UNKP-18-3-I-SZTE-66 to MT, UNKP-19-3-I-DE-186 GyD, UNKP-19-3-SZTE-318 to ÁV) and EFOP 3.6.3-VEKOP-16-2017-00009 to MT.

Acknowledgements

The authors are grateful to Yasuo Mori for generously providing the TRPM2 knockout mice. The authors are also grateful to Indu Ambudkar for the scientific discussions.

Translational Perspective

Inflammatory disorders of the pancreas (such as acute and chronic pancreatitis) pose a significant clinical challenge as currently no specific pharmaceutical treatment exists. Basic science studies can identify pathogenic disease mechanisms as novel drug targets, which can support drug discovery and therapy development in pancreatic diseases. Disturbed intracellular Ca^{2+} signalling caused by bile acids is a hallmark of the disease, which induces increased reactive oxygen species production, mitochondrial damage, intra-acinar digestive enzyme activation and cell death. Because of this mechanism of action, prevention of toxic cellular Ca^{2+} overload might be a promising therapeutic target. Transient Receptor Potential Melastatin 2 (TRPM2) is a non-selective cation channel that has recently emerged as an important contributor to oxidative-stress-induced cellular Ca^{2+} overload across different diseases. In our study, we are the first to report that TRPM2 is expressed in the acinar and

ductal cells of the exocrine pancreas, which can be activated by increased oxidative stress. Activation of TRPM2 contributed to bile acid-induced extracellular Ca^{2+} influx in acinar cells, which promoted necrosis *in vitro* and *in vivo*. In an experimental model of biliary acute pancreatitis genetic knockout of TRPM2 significantly decreased the disease severity and protected acinar cell. Based on these results we suggest that the inhibition of TRPM2 may be a potential treatment option for biliary pancreatitis and development of novel TRPM2 inhibitors can be translated to patients benefit.

References

Abuarab N, Munsey TS, Jiang LH, Li J & Sivaprasadarao A. (2017). High glucose-induced ROS activates TRPM2 to trigger lysosomal membrane permeabilization and Zn(2+)-mediated mitochondrial fission. *Sci Signal* **10**.

Ahuja M, Jha A, Maleth J, Park S & Muallem S. (2014). cAMP and Ca(2)(+) signaling in secretory epithelia: crosstalk and synergism. *Cell Calcium* **55,** 385-393.

Booth DM, Murphy JA, Mukherjee R, Awais M, Neoptolemos JP, Gerasimenko OV, Tepikin AV, Petersen OH, Sutton R & Criddle DN. (2011). Reactive oxygen species induced by bile acid induce apoptosis and protect against necrosis in pancreatic acinar cells. *Gastroenterology* **140,** 2116-2125.

Criddle DN, Murphy J, Fistetto G, Barrow S, Tepikin AV, Neoptolemos JP, Sutton R & Petersen OH. (2006). Fatty acid ethyl esters cause pancreatic calcium toxicity via inositol trisphosphate receptors and loss of ATP synthesis. *Gastroenterology* **130,** 781-793.

Di A, Gao XP, Qian F, Kawamura T, Han J, Hecquet C, Ye RD, Vogel SM & Malik AB. (2011). The redox-sensitive cation channel TRPM2 modulates phagocyte ROS production and inflammation. *Nat Immunol* **13,** 29-34.

DiMagno EP, Shorter RG, Taylor WF & Go VL. (1982). Relationships between pancreaticobiliary ductal anatomy and pancreatic ductal and parenchymal histology. *Cancer* **49,** 361-368.

Gerasimenko JV, Flowerdew SE, Voronina SG, Sukhomlin TK, Tepikin AV, Petersen OH & Gerasimenko OV. (2006). Bile acids induce Ca2+ release from both the endoplasmic reticulum and acidic intracellular calcium stores through activation of inositol trisphosphate receptors and ryanodine receptors. *J Biol Chem* **281,** 40154-40163.

Gerasimenko JV, Gryshchenko O, Ferdek PE, Stapleton E, Hebert TO, Bychkova S, Peng S, Begg M, Gerasimenko OV & Petersen OH. (2013). Ca2+ release-activated Ca2+ channel blockade as a potential tool in antipancreatitis therapy. *Proc Natl Acad Sci U S A* **110,** 13186-13191.

Geyer N, Diszhazi G, Csernoch L, Jona I & Almassy J. (2015). Bile acids activate ryanodine receptors in pancreatic acinar cells via a direct allosteric mechanism. *Cell Calcium* **58,** 160-170.

Gout J, Pommier RM, Vincent DF, Kaniewski B, Martel S, Valcourt U & Bartholin L. (2013). Isolation and culture of mouse primary pancreatic acinar cells. *J Vis Exp*.

Halangk W, Kruger B, Ruthenburger M, Sturzebecher J, Albrecht E, Lippert H & Lerch MM. (2002). Trypsin activity is not involved in premature, intrapancreatic trypsinogen activation. *Am J Physiol Gastrointest Liver Physiol* **282,** G367-374.

Hara Y, Wakamori M, Ishii M, Maeno E, Nishida M, Yoshida T, Yamada H, Shimizu S, Mori E, Kudoh J, Shimizu N, Kurose H, Okada Y, Imoto K & Mori Y. (2002). LTRPC2 Ca2+-permeable channel activated by changes in redox status confers susceptibility to cell death. *Mol Cell* **9,** 163-173.

Hegyi P, Rakonczay Z, Jr., Gray MA & Argent BE. (2004). Measurement of intracellular pH in pancreatic duct cells: a new method for calibrating the fluorescence data. *Pancreas* **28,** 427-434.

Hong JH, Li Q, Kim MS, Shin DM, Feske S, Birnbaumer L, Cheng KT, Ambudkar IS & Muallem S. (2011). Polarized but differential localization and recruitment of STIM1, Orai1 and TRPC channels in secretory cells. *Traffic* **12,** 232-245.

Kashio M, Sokabe T, Shintaku K, Uematsu T, Fukuta N, Kobayashi N, Mori Y & Tominaga M. (2012). Redox signal-mediated sensitization of transient receptor potential melastatin 2 (TRPM2) to temperature affects macrophage functions. *Proc Natl Acad Sci U S A* **109,** 6745-6750.

Kim JY, Kim KH, Lee JA, Namkung W, Sun AQ, Ananthanarayanan M, Suchy FJ, Shin DM, Muallem S & Lee MG. (2002). Transporter-mediated bile acid uptake causes Ca2+-dependent cell death in rat pancreatic acinar cells. *Gastroenterology* **122,** 1941-1953.

Kim MS, Hong JH, Li Q, Shin DM, Abramowitz J, Birnbaumer L & Muallem S. (2009). Deletion of TRPC3 in mice reduces store-operated Ca2+ influx and the severity of acute pancreatitis. *Gastroenterology* **137,** 1509-1517.

Kruger B, Albrecht E & Lerch MM. (2000). The role of intracellular calcium signaling in premature protease activation and the onset of pancreatitis. *Am J Pathol* **157,** 43-50.

Lerch MM & Aghdassi AA. (2010). The role of bile acids in gallstone-induced pancreatitis. *Gastroenterology* **138,** 429-433.

Lerch MM, Saluja AK, Runzi M, Dawra R, Saluja M & Steer ML. (1993). Pancreatic duct obstruction triggers acute necrotizing pancreatitis in the opossum. *Gastroenterology* **104,** 853-861.

Liu X, Cotrim A, Teos L, Zheng C, Swaim W, Mitchell J, Mori Y & Ambudkar I. (2013). Loss of TRPM2 function protects against irradiation-induced salivary gland dysfunction. *Nat Commun* **4,** 1515.

Liu X, Gong B, de Souza LB, Ong HL, Subedi KP, Cheng KT, Swaim W, Zheng C, Mori Y & Ambudkar IS. (2017). Radiation inhibits salivary gland function by promoting STIM1 cleavage by caspase-3 and loss of SOCE through a TRPM2-dependent pathway. *Sci Signal* **10**.

Maleth J, Balazs A, Pallagi P, Balla Z, Kui B, Katona M, Judak L, Nemeth I, Kemeny LV, Rakonczay Z, Jr., Venglovecz V, Foldesi I, Peto Z, Somoracz A, Borka K, Perdomo D, Lukacs GL, Gray MA, Monterisi S, Zaccolo M, Sendler M, Mayerle J, Kuhn JP, Lerch MM, Sahin-Toth M & Hegyi P. (2015). Alcohol disrupts levels and function of the cystic fibrosis transmembrane conductance regulator to promote development of pancreatitis. *Gastroenterology* **148,** 427-439 e416.

Maleth J & Hegyi P. (2014). Calcium signaling in pancreatic ductal epithelial cells: an old friend and a nasty enemy. *Cell Calcium* **55,** 337-345.

Maleth J, Venglovecz V, Razga Z, Tiszlavicz L, Rakonczay Z, Jr. & Hegyi P. (2011). Non-conjugated chenodeoxycholate induces severe mitochondrial damage and inhibits bicarbonate transport in pancreatic duct cells. *Gut* **60,** 136-138.

Manna PT, Munsey TS, Abuarab N, Li F, Asipu A, Howell G, Sedo A, Yang W, Naylor J, Beech DJ, Jiang LH & Sivaprasadarao A. (2015). TRPM2-mediated intracellular Zn2+ release triggers pancreatic beta-cell death. *Biochem J* **466,** 537-546.

Miller BA, Wang J, Song J, Zhang XQ, Hirschler-Laszkiewicz I, Shanmughapriya S, Tomar D, Rajan S, Feldman AM, Madesh M, Sheu SS & Cheung JY. (2019). Trpm2 enhances physiological bioenergetics and protects against pathological oxidative cardiac injury: Role of Pyk2 phosphorylation. *J Cell Physiol*.

Molnar R, Madacsy T, Varga A, Nemeth M, Katona X, Gorog M, Molnar B, Fanczal J, Rakonczay Z, Jr., Hegyi P, Pallagi P & Maleth J. (2019). Mouse pancreatic ductal organoid culture as a relevant model to study exocrine pancreatic ion secretion. *Lab Invest*.

Muili KA, Jin S, Orabi AI, Eisses JF, Javed TA, Le T, Bottino R, Jayaraman T & Husain SZ. (2013a). Pancreatic acinar cell nuclear factor kappaB activation because of bile acid exposure is dependent on calcineurin. *J Biol Chem* **288,** 21065-21073.

Muili KA, Wang D, Orabi AI, Sarwar S, Luo Y, Javed TA, Eisses JF, Mahmood SM, Jin S, Singh VP, Ananthanaravanan M, Perides G, Williams JA, Molkentin JD & Husain SZ. (2013b). Bile acids induce pancreatic acinar cell injury and pancreatitis by activating calcineurin. *J Biol Chem* **288,** 570-580.

Pallagi P, Balla Z, Singh AK, Dosa S, Ivanyi B, Kukor Z, Toth A, Riederer B, Liu Y, Engelhardt R, Jarmay K, Szabo A, Janovszky A, Perides G, Venglovecz V, Maleth J, Wittmann T, Takacs T, Gray MA, Gacser A, Hegyi P, Seidler U & Rakonczay Z, Jr. (2014). The role of pancreatic ductal secretion in protection against acute pancreatitis in mice*. *Crit Care Med* **42,** e177-188.

Park MK, Ashby MC, Erdemli G, Petersen OH & Tepikin AV. (2001). Perinuclear, perigranular and sub-plasmalemmal mitochondria have distinct functions in the regulation of cellular calcium transport. *EMBO J* **20,** 1863-1874.

Parniczky A, Kui B, Szentesi A, Balazs A, Szucs A, Mosztbacher D, Czimmer J, Sarlos P, Bajor J, Godi S, Vincze A, Illes A, Szabo I, Par G, Takacs T, Czako L, Szepes Z, Rakonczay Z, Izbeki F, Gervain J, Halasz A, Novak J, Crai S, Hritz I, Gog C, Sumegi J, Golovics P, Varga M, Bod B, Hamvas J, Varga-Muller M, Papp Z, Sahin-Toth M & Hegyi P. (2016). Prospective, Multicentre, Nationwide Clinical Data from 600 Cases of Acute Pancreatitis. *PLoS One* **11,** e0165309.

Perides G, Laukkarinen JM, Vassileva G & Steer ML. (2010a). Biliary acute pancreatitis in mice is mediated by the G-protein-coupled cell surface bile acid receptor Gpbar1. *Gastroenterology* **138,** 715-725.

Perides G, van Acker GJ, Laukkarinen JM & Steer ML. (2010b). Experimental acute biliary pancreatitis induced by retrograde infusion of bile acids into the mouse pancreatic duct. *Nat Protoc* **5,** 335-341.

Perraud AL, Takanishi CL, Shen B, Kang S, Smith MK, Schmitz C, Knowles HM, Ferraris D, Li W, Zhang J, Stoddard BL & Scharenberg AM. (2005). Accumulation of free ADP-ribose from mitochondria mediates oxidative stress-induced gating of TRPM2 cation channels. *J Biol Chem* **280,** 6138-6148.

Schulz S, Schmitt S, Wimmer R, Aichler M, Eisenhofer S, Lichtmannegger J, Eberhagen C, Artmann R, Tookos F, Walch A, Krappmann D, Brenner C, Rust C & Zischka H. (2013). Progressive stages of mitochondrial destruction caused by cell toxic bile salts. *Biochim Biophys Acta* **1828,** 2121-2133.

Sendler M, van den Brandt C, Glaubitz J, Wilden A, Golchert J, Weiss FU, Homuth G, De Freitas Chama LL, Mishra N, Mahajan UM, Bossaller L, Volker U, Broker BM, Mayerle J & Lerch MM. (2019). NLRP3 Inflammasome Regulates Development of Systemic Inflammatory Respoes in Mice With Acute Pancreatitis. *Gastroenterology*.

Sendler M, Weiss FU, Golchert J, Homuth G, van den Brandt C, Mahajan UM, Partecke LI, Doring P, Gukovsky I, Gukovskaya AS, Wagh PR, Lerch MM & Mayerle J. (2018). Cathepsin B-Mediated Activation of Trypsinogen in Endocytosing Macrophages Increases Severity of Pancreatitis in Mice. *Gastroenterology* **154,** 704-718 e710.

Sherwood MW, Prior IA, Voronina SG, Barrow SL, Woodsmith JD, Gerasimenko OV, Petersen OH & Tepikin AV. (2007). Activation of trypsinogen in large endocytic vacuoles of pancreatic acinar cells. *Proc Natl Acad Sci U S A* **104,** 5674-5679.

Sousa T, Castro RE, Pinto SN, Coutinho A, Lucas SD, Moreira R, Rodrigues CM, Prieto M & Fernandes F. (2015). Deoxycholic acid modulates cell death signaling through changes in mitochondrial membrane properties. *J Lipid Res* **56,** 2158-2171.

Takahashi N, Kozai D, Kobayashi R, Ebert M & Mori Y. (2011). Roles of TRPM2 in oxidative stress. *Cell Calcium* **50,** 279-287.

Tsutsui M, Hirase R, Miyamura S, Nagayasu K, Nakagawa T, Mori Y, Shirakawa H & Kaneko S. (2018). TRPM2 Exacerbates Central Nervous System Inflammation in Experimental Autoimmune Encephalomyelitis by Increasing Production of CXCL2 Chemokines. *J Neurosci* **38,** 8484-8495.

Uchida K, Dezaki K, Damdindorj B, Inada H, Shiuchi T, Mori Y, Yada T, Minokoshi Y & Tominaga M. (2011). Lack of TRPM2 impaired insulin secretion and glucose metabolisms in mice. *Diabetes* **60,** 119-126.

Venglovecz V, Rakonczay Z, Jr., Ozsvari B, Takacs T, Lonovics J, Varro A, Gray MA, Argent BE & Hegyi P. (2008). Effects of bile acids on pancreatic ductal bicarbonate secretion in guinea pig. *Gut* **57,** 1102-1112.

Voronina SG, Barrow SL, Gerasimenko OV, Petersen OH & Tepikin AV. (2004). Effects of secretagogues and bile acids on mitochondrial membrane potential of pancreatic acinar cells: comparison of different modes of evaluating DeltaPsim. *Journal of Biological Chemistry* **279,** 27327-27338.

Voronina SG, Barrow SL, Simpson AW, Gerasimenko OV, da Silva Xavier G, Rutter GA, Petersen OH & Tepikin AV. (2010). Dynamic changes in cytosolic and mitochondrial ATP levels in pancreatic acinar cells. *Gastroenterology* **138,** 1976-1987.

Wen L, Voronina S, Javed MA, Awais M, Szatmary P, Latawiec D, Chvanov M, Collier D, Huang W, Barrett J, Begg M, Stauderman K, Roos J, Grigoryev S, Ramos S, Rogers E, Whitten J, Velicelebi G, Dunn M, Tepikin AV, Criddle DN & Sutton R. (2015). Inhibitors of ORAI1 Prevent Cytosolic Calcium-Associated Injury of Human Pancreatic Acinar Cells and Acute Pancreatitis in 3 Mouse Models. *Gastroenterology* **149,** 481-492 e487.

Yadav D & Lowenfels AB. (2013). The epidemiology of pancreatitis and pancreatic cancer. *Gastroenterology* **144,** 1252-1261.

Yamamoto S, Shimizu S, Kiyonaka S, Takahashi N, Wajima T, Hara Y, Negoro T, Hiroi T, Kiuchi Y, Okada T, Kaneko S, Lange I, Fleig A, Penner R, Nishi M, Takeshima H & Mori Y. (2008). TRPM2-mediated Ca2+influx induces chemokine production in monocytes that aggravates inflammatory neutrophil infiltration. *Nat Med* **14,** 738-747.

Figure 1. Expression of TRPM2 in the exocrine pancreas. A. Agarose gel images of cDNA samples derived from isolated acini and ductal fragments confirmed that the TRPM2 gene is expressed in the exocrine pancreas. **B–C.** Immunofluorescent labelling of TRPM2 on isolated acinar clusters and cross sections of isolated ducts. TRPM2 channels are expressed on the basolateral membrane of the pancreatic acinar cells and on the apical membrane in ductal cells, which is also demonstrated on the transmitted light images Scale bar: 10 μm

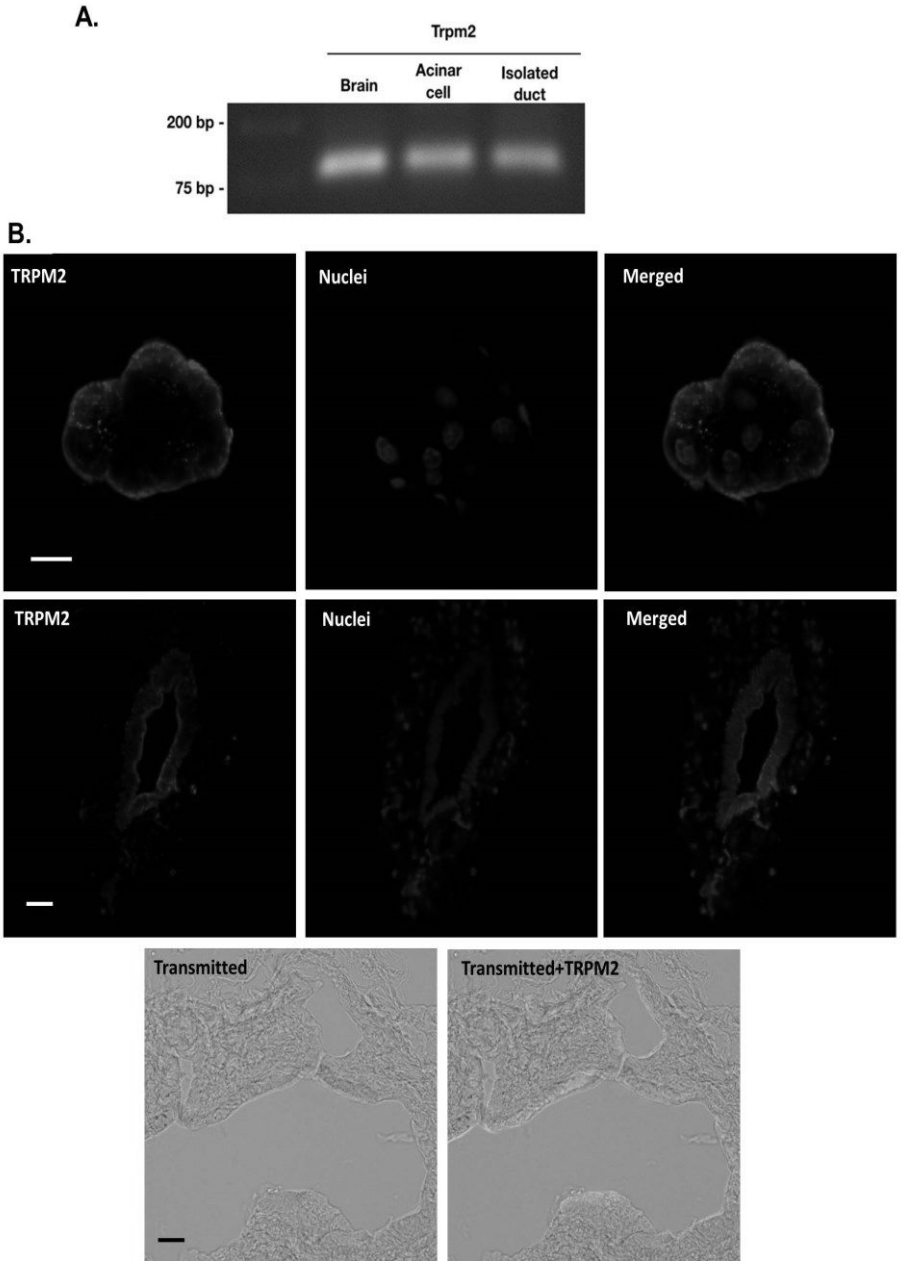

Figure 2. Functional activity of TRPM2 in the exocrine pancreas. A. Average traces of 5–6 individual experiments demonstrating the effect of 1 mM H_2O_2 on pancreatic acinar cells in the presence or absence of extracellular Ca^{2+}. Bar charts summarise the maximal Ca^{2+} responses to H_2O_2, which was significantly reduced in TRPM2 KO acini. *: $p < 0.05$ vs WT. **B.** Representative whole cell current recordings and current–voltage relationships in isolated pancreatic acini. H_2O_2 activated a reversible cationic membrane current, with a relative linear I–V relationship. n = 4/group. **C.** Averages of intracellular Ca^{2+} recordings in isolated pancreatic ducts (5–6 experiments/group) in the presence or absence of extracellular Ca^{2+}. The intracellular Ca^{2+} level decreases in response to extracellular Ca^{2+} removal as demonstrated by the rrepresentative trace of intracellular Ca^{2+} recordings in isolated pancreatic duct (wild type). Bar charts summarise the maximal Ca^{2+} elevations evoked by H_2O_2, which was significantly lower in TRPM2 KO ductal cells. These results suggest that TRPM2 mediates extracellular Ca^{2+} influx under an oxidative stress condition in pancreatic acinar and ductal cells. *: $p < 0.05$ vs WT.

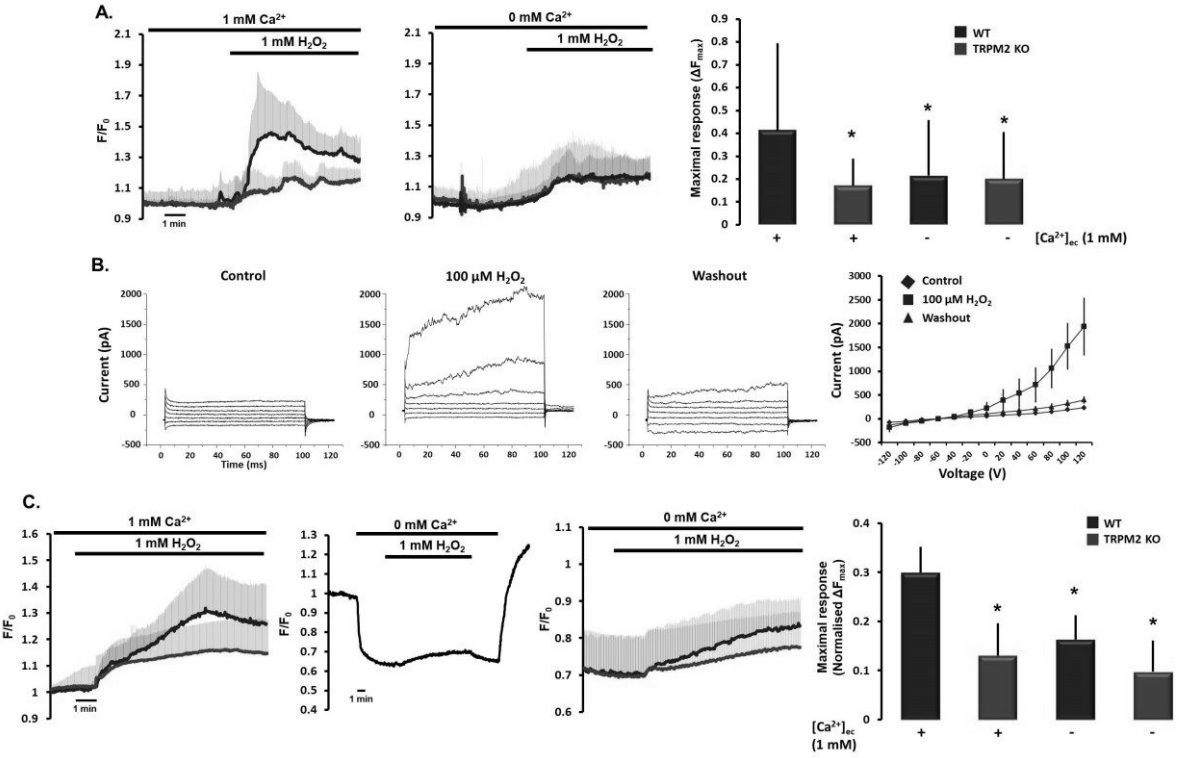

Figure 3. The role of TRPM2 in bile-acid-evoked Ca^{2+} signal generation. A–B. Average traces and bar charts of 5–6 individual experiments comparing intracellular Ca^{2+} elevations evoked by 250 μM CDC in WT and TRPM2 KO acini and isolated ducts. Genetic deletion of TRPM2 reduced the bile-acid-induced Ca^{2+} elevation in pancreatic acini, but not in ducts. *: $p < 0.05$ vs WT. **C.** Average pH_i traces of 4–6 experiments for each condition. Pancreatic ducts were perfused with HCO_3^-/CO_2-buffered extracellular solution, and intracellular alkalisation was achieved by 20 mM NH_4Cl administration. **D.** Bar charts of the calculated base fluxes of HCO_3^-. 250 μM CDC significantly decreased both alkaline and acidic recovery; however, no significant difference was detected in WT and TRPM2 KO ducts. **E.** Average traces of H2DCFDA intensities and bar charts of the maximal fluorescent intensity changes in isolated acini and ducts. ROS generation induced by bile acid treatment was measured in 5–6 individual experiments. *: $p < 0.05$ vs acini.

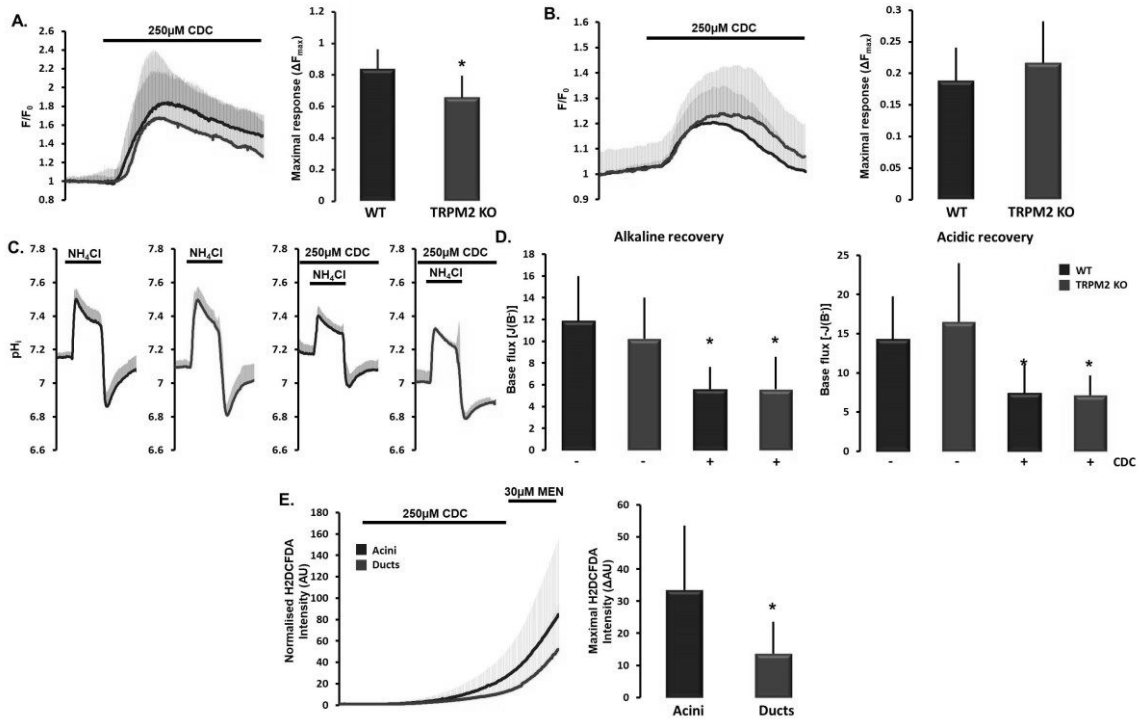

Figure 4. The role of TRPM2 in acinar cell necrosis during bile acid exposure. A. Representative images of different conditions (blue: live cells labelled with CytoCalcein 450, green: necrotic cells labelled with Nuclear Green, and red: apoptotic cells labelled with Apopxin Deep Red). Scale bar: 20 µm. **B.** Bar chart representing the ratio of live, apoptotic and necrotic cells. Incubation of WT and TRPM2 KO acini with 1 mM H_2O_2 or with 250 µM CDC for 30 min markedly decreased the number of viable cells, whereas necrosis was significantly increased. TRPM2 KO acinar cells displayed a significantly decreased rate of apoptosis in the bile acid treated group, whereas cell necrosis was impaired in both cases. n: 4-5 experiment/group. **C.** Bar charts representing the ratio of live, apoptotic and necrotic cells. TRPM2 knockout significantly improved acinar cell survival in 1 mM H_2O_2 or with 250 µM CDC treated groups. *: $p< 0.05$ vs WT treated sample (H_2O_2 or CDC); n: 4-5 experiment/group.

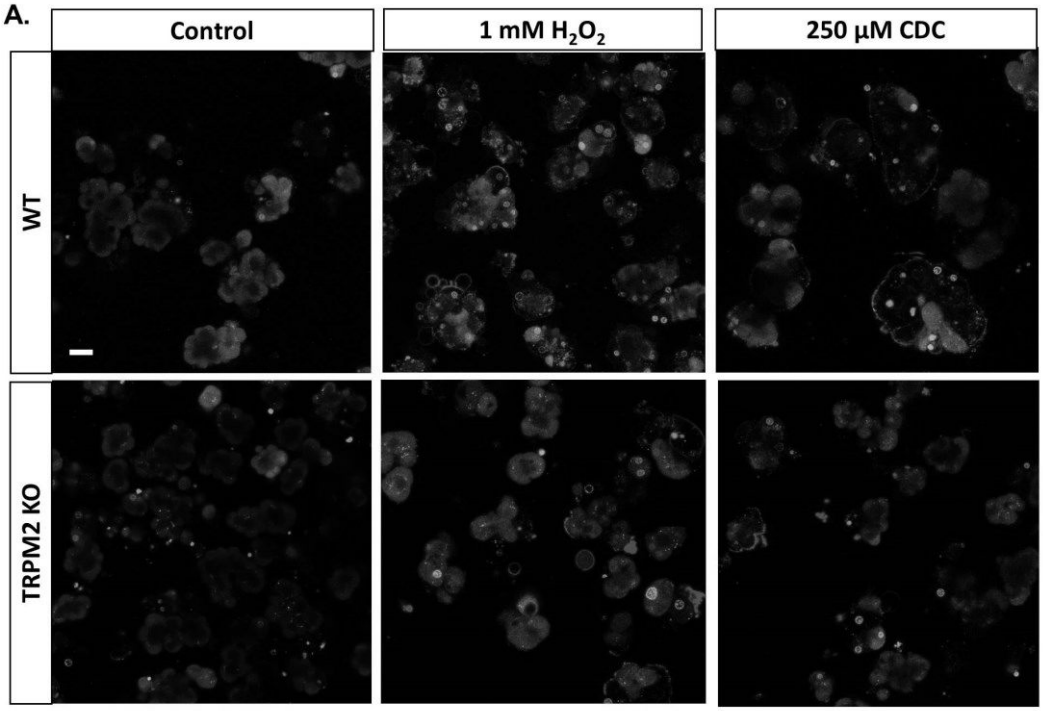

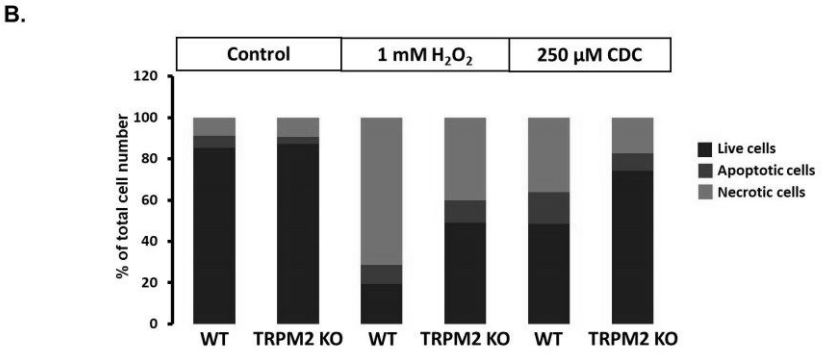

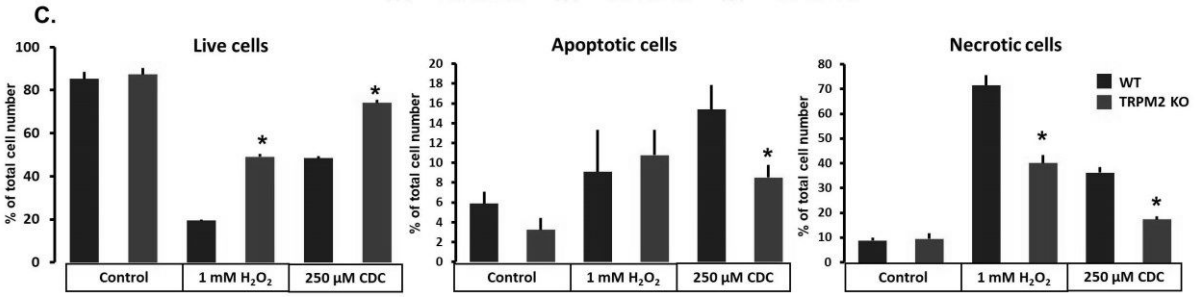

Figure 5. The effect of TRPM2 on the development of mitochondrial damage. A. Average traces and bar charts of the changes of $\Delta\psi_m$ in WT and TRPM2 pancreatic acinar cells. 1 mM H_2O_2 markedly decreased $\Delta\psi_m$ in WT cells (blue trace), which was impaired by TRPM2 knockout (red trace) or removal of the extracellular Ca^{2+} (green trace). For control cells were perfused with standard HEPES solution (grey trace). **B.** By contrast, no difference was observed when acinar cells were challenged by 250 µM CDC. **C.** Representative confocal images of labelled mitochondria in pancreatic acinar cells. Mitochondrial fragmentation was not observed in response to H_2O_2, or to bile acid treatment. Scale bar: 10 µm. n: 6–7 experiments/groups; *: $p < 0.05$ vs WT.

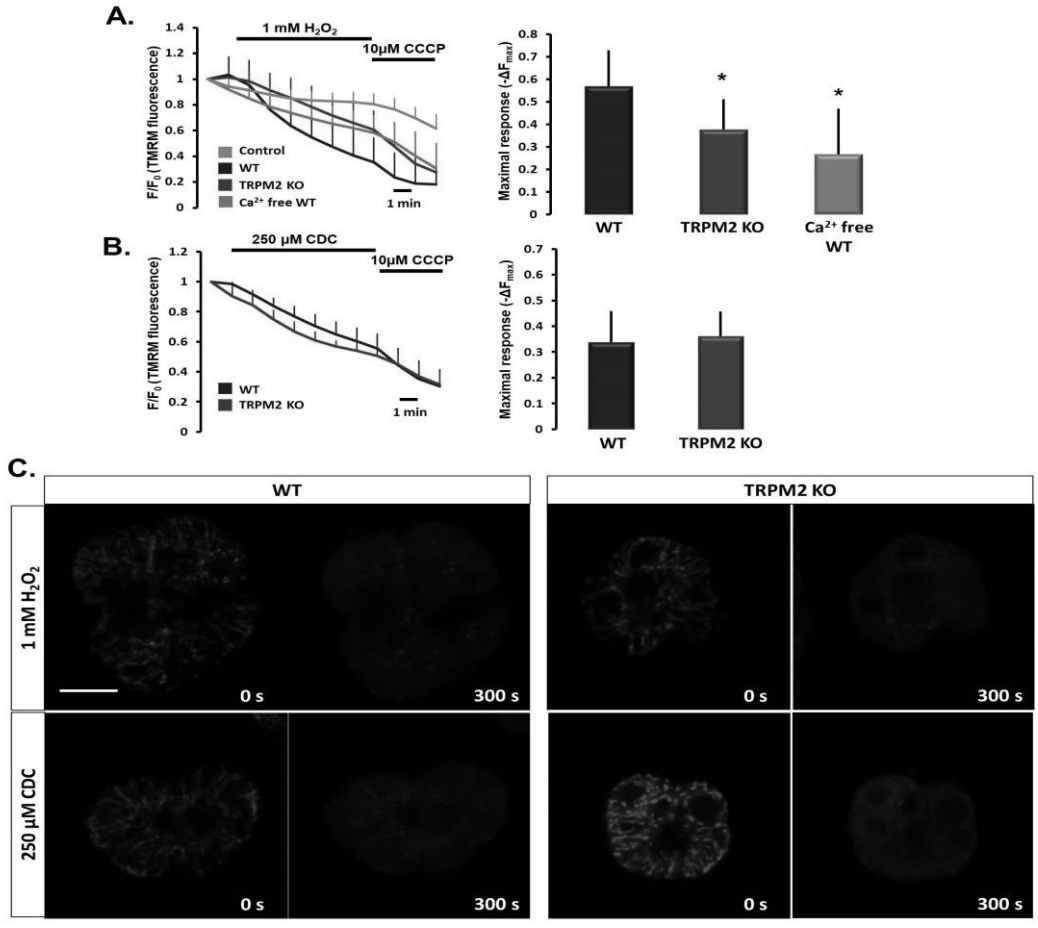

Figure 6. Genetic knockout of TRPM2 decreases the severity of biliary, but not cerulein-induced, acute pancreatitis. A. Representative images of pancreatic histology in cerulein-induced pancreatitis. Mice were given 10 hourly i.p. injections of either physiological saline (control group) or 50 μg/bwkg cerulein. Scale bar: 100 μm. **B.** Cerulein administration caused extensive pancreatic damage; however, no significant differences were observed in the histological parameters of WT and TRPM2 KO animals. n: 6–7 animals/groups; *: $p < 0.05$ vs WT; **: $p < 0.05$ vs TRPM2 KO. **C.** Representative images of pancreatic histology in Na-taurocholate-induced pancreatitis. Pancreatitis was induced by intraductal infusion of 4% Na-taurocholate (TC). Scale bar: 100 μm. **D.** The infusion of 4% Na-taurocholate-induced necrotising pancreatitis in WT and TRPM2 KO mice accompanied by elevated histological and laboratory parameters. Although the extent of interstitial oedema or leukocyte infiltration was not different, the extent of necrosis was significantly impaired in the TRPM2 KO animals. n: 6–7 animals/groups; *: $p < 0.05$ vs WT control; **: $p < 0.05$ vs TRPM2 KO control; a: $p < 0.05$ vs WT Na-TC treated.